10-14-2004

Underlying event in hard interactions at the Fermilab Tevatron $\bar{p}p$ collider

Darin Acosta
University of Florida, acosta@phys.ufl.edu

Kenneth A. Bloom
University of Nebraska-Lincoln, kenbloom@unl.edu

Collider Detector at Fermilab Collaboration

Underlying event in hard interactions at the Fermilab Tevatron $\bar{p}p$ collider

D. Acosta,[14] T. Affolder,[7] M. G. Albrow,[13] D. Ambrose,[36] D. Amidei,[27] K. Anikeev,[26] J. Antos,[1] G. Apollinari,[13] T. Arisawa,[50] A. Artikov,[11] W. Ashmanskas,[2] F. Azfar,[34] P. Azzi-Bacchetta,[35] N. Bacchetta,[35] H. Bachacou,[24] W. Badgett,[13] A. Barbaro-Galtieri,[24] V. E. Barnes,[39] B. A. Barnett,[21] S. Baroiant,[5] M. Barone,[15] G. Bauer,[26] F. Bedeschi,[37] S. Behari,[21] S. Belforte,[47] W. H. Bell,[17] G. Bellettini,[37] J. Bellinger,[51] D. Benjamin,[12] A. Beretvas,[13] A. Bhatti,[41] M. Binkley,[13] D. Bisello,[35] M. Bishai,[13] R. E. Blair,[2] C. Blocker,[4] K. Bloom,[27] B. Blumenfeld,[21] A. Bocci,[41] A. Bodek,[40] G. Bolla,[39] A. Bolshov,[26] D. Bortoletto,[39] J. Boudreau,[38] C. Bromberg,[28] E. Brubaker,[24] J. Budagov,[11] H. S. Budd,[40] K. Burkett,[13] G. Busetto,[35] K. L. Byrum,[2] S. Cabrera,[12] M. Campbell,[27] W. Carithers,[24] D. Carlsmith,[51] A. Castro,[3] D. Cauz,[47] A. Cerri,[24] L. Cerrito,[20] J. Chapman,[27] C. Chen,[36] Y. C. Chen,[1] M. Chertok,[5] G. Chiarelli,[37] G. Chlachidze,[13] F. Chlebana,[13] M. L. Chu,[1] J. Y. Chung,[32] W.-H. Chung,[51] Y. S. Chung,[40] C. I. Ciobanu,[20] A. G. Clark,[16] M. Coca,[40] A. Connolly,[24] M. Convery,[41] J. Conway,[43] M. Cordelli,[15] J. Cranshaw,[45] R. Culbertson,[13] D. Dagenhart,[4] S. D'Auria,[17] P. de Barbaro,[40] S. De Cecco,[42] S. Dell'Agnello,[15] M. Dell'Orso,[37] S. Demers,[40] L. Demortier,[41] M. Deninno,[3] D. De Pedis,[42] P. F. Derwent,[13] C. Dionisi,[42] J. R. Dittmann,[13] A. Dominguez,[24] S. Donati,[37] M. D'Onofrio,[16] T. Dorigo,[35] N. Eddy,[20] R. Erbacher,[13] D. Errede,[20] S. Errede,[20] R. Eusebi,[40] S. Farrington,[17] R. G. Feild,[14] J. P. Fernandez,[39] C. Ferretti,[27] R. D. Field,[14] I. Fiori,[37] B. Flaugher,[13] L. R. Flores-Castillo,[38] G. W. Foster,[13] M. Franklin,[18] J. Friedman,[26] I. Furic,[26] M. Gallinaro,[41] M. Garcia-Sciveres,[24] A. F. Garfinkel,[39] C. Gay,[52] D. W. Gerdes,[27] E. Gerstein,[9] S. Giagu,[42] P. Giannetti,[37] K. Giolo,[39] M. Giordani,[47] P. Giromini,[15] V. Glagolev,[11] D. Glenzinski,[13] M. Gold,[30] N. Goldschmidt,[27] J. Goldstein,[34] G. Gomez,[8] M. Goncharov,[44] I. Gorelov,[30] A. T. Goshaw,[12] Y. Gotra,[38] K. Goulianos,[41] A. Gresele,[3] C. Grosso-Pilcher,[10] M. Guenther,[39] J. Guimaraes da Costa,[18] C. Haber,[24] S. R. Hahn,[13] E. Halkiadakis,[40] R. Handler,[51] F. Happacher,[15] K. Hara,[48] R. M. Harris,[13] F. Hartmann,[22] K. Hatakeyama,[41] J. Hauser,[6] J. Heinrich,[36] M. Hennecke,[22] M. Herndon,[21] C. Hill,[7] A. Hocker,[40] K. D. Hoffman,[10] S. Hou,[1] B. T. Huffman,[34] R. Hughes,[32] J. Huston,[28] C. Issever,[7] J. Incandela,[7] G. Introzzi,[37] M. Iori,[42] A. Ivanov,[40] Y. Iwata,[19] B. Iyutin,[26] E. James,[13] M. Jones,[39] T. Kamon,[44] J. Kang,[27] M. Karagoz Unel,[31] S. Kartal,[13] H. Kasha,[52] Y. Kato,[33] R. D. Kennedy,[13] R. Kephart,[13] B. Kilminster,[40] D. H. Kim,[23] H. S. Kim,[20] M. J. Kim,[9] S. B. Kim,[23] S. H. Kim,[48] T. H. Kim,[26] Y. K. Kim,[10] M. Kirby,[12] L. Kirsch,[4] S. Klimenko,[14] P. Koehn,[32] K. Kondo,[50] J. Konigsberg,[14] A. Korn,[26] A. Korytov,[14] J. Kroll,[36] M. Kruse,[12] V. Krutelyov,[44] S. E. Kuhlmann,[2] N. Kuznetsova,[13] A. T. Laasanen,[39] S. Lami,[41] S. Lammel,[13] J. Lancaster,[12] K. Lannon,[32] M. Lancaster,[25] R. Lander,[5] A. Lath,[43] G. Latino,[30] T. LeCompte,[2] Y. Le,[21] J. Lee,[40] S. W. Lee,[44] N. Leonardo,[26] S. Leone,[37] J. D. Lewis,[13] K. Li,[52] C. S. Lin,[13] M. Lindgren,[6] T. M. Liss,[20] T. Liu,[13] D. O. Litvintsev,[13] N. S. Lockyer,[36] A. Loginov,[29] M. Loreti,[35] D. Lucchesi,[35] P. Lukens,[13] L. Lyons,[34] J. Lys,[24] R. Madrak,[18] K. Maeshima,[13] P. Maksimovic,[21] L. Malferrari,[3] M. Mangano,[37] G. Manca,[34] M. Mariotti,[35] M. Martin,[21] A. Martin,[52] V. Martin,[31] M. Martínez,[13] P. Mazzanti,[3] K. S. McFarland,[40] P. McIntyre,[44] M. Menguzzato,[35] A. Menzione,[37] P. Merkel,[13] C. Mesropian,[41] A. Meyer,[13] T. Miao,[13] R. Miller,[28] J. S. Miller,[27] S. Miscetti,[15] G. Mitselmakher,[14] N. Moggi,[3] R. Moore,[13] T. Moulik,[39] M. Mulhearn,[26] A. Mukherjee,[13] T. Muller,[22] A. Munar,[36] P. Murat,[13] J. Nachtman,[13] S. Nahn,[52] I. Nakano,[19] R. Napora,[21] F. Niell,[27] C. Nelson,[13] T. Nelson,[13] C. Neu,[32] M. S. Neubauer,[26] C. Newman-Holmes,[13] T. Nigmanov,[38] L. Nodulman,[2] S. H. Oh,[12] Y. D. Oh,[23] T. Ohsugi,[19] T. Okusawa,[33] W. Orejudos,[24] C. Pagliarone,[37] F. Palmonari,[37] R. Paoletti,[37] V. Papadimitriou,[45] J. Patrick,[13] G. Pauletta,[47] M. Paulini,[9] T. Pauly,[34] C. Paus,[26] D. Pellett,[5] A. Penzo,[47] T. J. Phillips,[12] G. Piacentino,[37] J. Piedra,[8] K. T. Pitts,[20] A. Pompoš,[39] L. Pondrom,[51] G. Pope,[38] T. Pratt,[34] F. Prokoshin,[11] J. Proudfoot,[2] F. Ptohos,[15] O. Poukhov,[11] G. Punzi,[37] J. Rademacker,[34] A. Rakitine,[26] F. Ratnikov,[43] H. Ray,[27] A. Reichold,[34] P. Renton,[34] M. Rescigno,[42] F. Rimondi,[3] L. Ristori,[37] W. J. Robertson,[12] T. Rodrigo,[8] S. Rolli,[49] L. Rosenson,[26] R. Roser,[13] R. Rossin,[35] C. Rott,[39] A. Roy,[39] A. Ruiz,[8] D. Ryan,[49] A. Safonov,[5] R. St. Denis,[17] W. K. Sakumoto,[40] D. Saltzberg,[6] C. Sanchez,[32] A. Sansoni,[15] L. Santi,[47] S. Sarkar,[42] P. Savard,[46] A. Savoy-Navarro,[13] P. Schlabach,[13] E. E. Schmidt,[13] M. P. Schmidt,[13] M. Schmitt,[52] L. Scodellaro,[35] A. Scribano,[37] A. Sefov,[39] S. Seidel,[30] Y. Seiya,[48] A. Semenov,[11] F. Semeria,[3] M. D. Shapiro,[24] P. F. Shepard,[38] T. Shibayama,[48] M. Shimojima,[48] M. Shochet,[10] A. Sidoti,[35] A. Sill,[45] P. Sinervo,[46] A. J. Slaughter,[52] K. Sliwa,[49] F. D. Snider,[13] R. Snihur,[25] M. Spezziga,[45] F. Spinella,[37] M. Spiropulu,[7] L. Spiegel,[13] A. Stefanini,[37] J. Strologas,[30] D. Stuart,[7] A. Sukhanov,[14] K. Sumorok,[26] T. Suzuki,[48] R. Takashima,[19] K. Takikawa,[48] M. Tanaka,[2] V. Tano,[28] M. Tecchio,[27] R. J. Tesarek,[13] P. K. Teng,[1] K. Terashi,[41] S. Tether,[26] J. Thom,[13] A. S. Thompson,[17] E. Thomson,[32] P. Tipton,[40] S. Tkaczyk,[13] D. Toback,[44] K. Tollefson,[28] D. Tonelli,[37] M. Tönnesmann,[28] H. Toyoda,[33] W. Trischuk,[46] J. Tseng,[26] D. Tsybychev,[14] N. Turini,[37] F. Ukegawa,[48] T. Unverhau,[17] T. Vaiciulis,[40] A. Varganov,[27] E. Vataga,[37] S. Vejcik III,[13] G. Velev,[13] G. Veramendi,[24] R. Vidal,[13] I. Vila,[8] R. Vilar,[8] I. Volobouev,[24] M. von der Mey,[6] R. G. Wagner,[2]

R. L. Wagner,[13] W. Wagner,[22] Z. Wan,[43] C. Wang,[12] M. J. Wang,[1] S. M. Wang,[14] B. Ward,[17] S. Waschke,[17] D. Waters,[25] T. Watts,[43] M. Weber,[24] W. C. Wester III,[13] B. Whitehouse,[49] A. B. Wicklund,[2] E. Wicklund,[13] H. H. Williams,[36] P. Wilson,[13] B. L. Winer,[32] S. Wolbers,[13] M. Wolter,[49] S. Worm,[43] X. Wu,[16] F. Würthwein,[26] U. K. Yang,[10] W. Yao,[24] G. P. Yeh,[13] K. Yi,[21] J. Yoh,[13] T. Yoshida,[33] I. Yu,[23] S. Yu,[36] J. C. Yun,[13] L. Zanello,[42] A. Zanetti,[47] F. Zetti,[24] and S. Zucchelli[3]

(CDF Collaboration)

[1] *Institute of Physics, Academia Sinica, Taipei, Taiwan 11529, Republic of China*
[2] *Argonne National Laboratory, Argonne, Illinois 60439, USA*
[3] *Istituto Nazionale di Fisica Nucleare, University of Bologna, I-40127 Bologna, Italy*
[4] *Brandeis University, Waltham, Massachusetts 02254, USA*
[5] *University of California at Davis, Davis, California 95616, USA*
[6] *University of California at Los Angeles, Los Angeles, California 90024, USA*
[7] *University of California at Santa Barbara, Santa Barbara, California 93106, USA*
[8] *Instituto de Fisica de Cantabria, CSIC-University of Cantabria, 39005 Santander, Spain*
[9] *Carnegie Mellon University, Pittsburgh, Pennsylvania 15213, USA*
[10] *Enrico Fermi Institute, University of Chicago, Chicago, Illinois 60637, USA*
[11] *Joint Institute for Nuclear Research, RU-141980 Dubna, Russia*
[12] *Duke University, Durham, North Carolina 27708*
[13] *Fermi National Accelerator Laboratory, Batavia, Illinois 60510, USA*
[14] *University of Florida, Gainesville, Florida 32611, USA*
[15] *Laboratori Nazionali di Frascati, Istituto Nazionale di Fisica Nucleare, I-00044 Frascati, Italy*
[16] *University of Geneva, CH-1211 Geneva 4, Switzerland*
[17] *Glasgow University, Glasgow G12 8QQ, United Kingdom*
[18] *Harvard University, Cambridge, Massachusetts 02138, USA*
[19] *Hiroshima University, Higashi-Hiroshima 724, Japan*
[20] *University of Illinois, Urbana, Illinois 61801, USA*
[21] *The Johns Hopkins University, Baltimore, Maryland 21218, USA*
[22] *Institut für Experimentelle Kernphysik, Universität Karlsruhe, 76128 Karlsruhe, Germany*
[23] *Center for High Energy Physics, Kyungpook National University, Taegu 702-701; Seoul National University, Seoul 151-742; SungKyunKwan University, Suwon 440-746, Korea*
[24] *Ernest Orlando Lawrence Berkeley National Laboratory, Berkeley, California 94720, USA*
[25] *University College London, London WC1E 6BT, United Kingdom*
[26] *Massachusetts Institute of Technology, Cambridge, Massachusetts 02139, USA*
[27] *University of Michigan, Ann Arbor, Michigan 48109, USA*
[28] *Michigan State University, East Lansing, Michigan 48824, USA*
[29] *Institution for Theoretical and Experimental Physics, ITEP, Moscow 117259, Russia*
[30] *University of New Mexico, Albuquerque, New Mexico 87131, USA*
[31] *Northwestern University, Evanston, Illinois 60208, USA*
[32] *The Ohio State University, Columbus, Ohio 43210, USA*
[33] *Osaka City University, Osaka 588, Japan*
[34] *University of Oxford, Oxford OX1 3RH, United Kingdom*
[35] *Universita di Padova, Istituto Nazionale di Fisica Nucleare, Sezione di Padova, I-35131 Padova, Italy*
[36] *University of Pennsylvania, Philadelphia, Pennsylvania 19104, USA*
[37] *Istituto Nazionale di Fisica Nucleare, University and Scuola Normale Superiore of Pisa, I-56100 Pisa, Italy*
[38] *University of Pittsburgh, Pittsburgh, Pennsylvania 15260, USA*
[39] *Purdue University, West Lafayette, Indiana 47907, USA*
[40] *University of Rochester, Rochester, New York 14627, USA*
[41] *Rockefeller University, New York, New York 10021, USA*
[42] *Instituto Nazionale de Fisica Nucleare, Sezione di Roma, University di Roma I, "La Sapienza," I-00185 Roma, Italy*
[43] *Rutgers University, Piscataway, New Jersey 08855, USA*
[44] *Texas A&M University, College Station, Texas 77843, USA*
[45] *Texas Tech University, Lubbock, Texas 79409, USA*
[46] *Institute of Particle Physics, University of Toronto, Toronto M5S 1A7, Canada*
[47] *Istituto Nazionale di Fisica Nucleare, University of Trieste, Udine, Italy*
[48] *University of Tsukuba, Tsukuba, Ibaraki 305, Japan*
[49] *Tufts University, Medford, Massachusetts 02155, USA*
[50] *Waseda University, Tokyo 169, Japan*

[51]*University of Wisconsin, Madison, Wisconsin 53706, USA*
[52]*Yale University, New Haven, Connecticut 06520, USA*
(Received 13 April 2004; published 14 October 2004)

For comparison of inclusive jet cross sections measured at hadron-hadron colliders to next-to-leading order (NLO) parton-level calculations, the energy deposited in the jet cone by spectator parton interactions must first be subtracted. The assumption made at the Tevatron is that the spectator parton interaction energy is similar to the ambient level measured in minimum bias events. In this paper, we test this assumption by measuring the ambient charged track momentum in events containing large transverse energy jets at $\sqrt{s} = 1800$ GeV and $\sqrt{s} = 630$ GeV and comparing this ambient momentum with that observed both in minimum bias events and with that predicted by two Monte Carlo models. Two cones in $\eta - \phi$ space are defined, at the same pseudorapidity, η, as the jet with the highest transverse energy ($E_T^{(1)}$), and at $\pm 90^o$ in the azimuthal direction, ϕ. The total charged track momentum inside each of the two cones is measured. The minimum momentum in the two cones is almost independent of $E_T^{(1)}$ and is similar to the momentum observed in minimum bias events, whereas the maximum momentum increases roughly linearly with the jet $E_T^{(1)}$ over most of the measured range. This study was carried out using data from the CDF detector taken during Run 1 (1994-1995). The study will help improve the precision of comparisons of jet cross section data and NLO perturbative QCD predictions. The distribution of the sum of the track momenta in the two cones is also examined for five different $E_T^{(1)}$ bins. The HERWIG and PYTHIA Monte Carlo generators are reasonably successful in describing the data, but neither can describe completely all of the event properties.

DOI: 10.1103/PhysRevD.70.072002 PACS numbers: 13.87.Fh

Jet production at hadron colliders, the highest energy probe in particle physics, has been used to measure parton distribution functions, the running of the strong coupling constant, α_s, and to search for new physics. At the Fermilab Tevatron $\bar{p}p$ collider, the jet production rate has been measured for jets of 15–450 GeV at $\sqrt{s} =$ 1800 GeV [1–8], and jets of 15–150 GeV at $\sqrt{s} =$ 630 GeV [9], [10]. The production of jets involves the interaction of an individual parton (quark or gluon) from one beam hadron with a parton from the other beam hadron. Each of the interacting partons carries only a fraction of the parent hadron's momentum with the residual momentum remaining with the other (spectator) constituents of the hadron. In addition, there are interactions between the spectator constituents of the two hadrons which normally occur at low momentum transfers. Measurements involving the observed jets are compared to perturbative QCD predictions. For NLO perturbative QCD predictions, only the parton-level cross section, i.e., the cross section of two partons producing either two or three partons in the final state, is calculated. After convolution with the parton distribution functions, this cross section is directly compared with experimental data. For these comparisons to be valid, the energy from spectator interactions, which may fall in the jet cone, must be subtracted from the experimentally observed jets. In hard interaction jet events, the energy outside the two primary jets consists of energy from spectator interactions (soft and semihard), initial and final state radiation and any hadronization leakage from the jet cones. Initial and final state radiation effects are part of higher order perturbative QCD calculations and at least a portion of these effects are already included in NLO calculations.

Because the CDF detector measures the momenta of low P_T tracks more accurately than the calorimeter measures their energies, we choose to work with the track momenta in our analysis. We will call the charged track momenta associated with spectator interactions the *underlying event momentum*. It is the momentum in an event which is not directly related to the hard interaction. Clearly, this is a working definition as a coupling exists between all aspects of a $\bar{p}p$ interaction. For example, the hadronization of the partons from the hard interaction and from the spectator interactions are ultimately linked as the final state hadrons must be colorless. In current QCD studies at hadron colliders, the underlying event energy in the jet events is assumed to be well approximated by the ambient energy in the events collected with minimal trigger requirements. Normally, these *minimum bias* events are triggered by presence of particles away from the beam in the forward and backward direction. The subtraction of the underlying event energy leads to the largest uncertainty in jet cross section measurement for $E_T \leq 50$ GeV [1]. A precise measurement of the spectator interaction energy is essential for the modeling/understanding of nonperturbative QCD effects and for any quantitative improvement of the jet studies. Another important question is whether the presence of a hard interaction in the event influences the spectator interactions.

The measurement of the momentum in minimum bias events is important in its own right as it is used to estimate the effect of multiple interaction events on any signal at hadron colliders, where, due to high instantaneous luminosity, several interactions may occur in the same bunch crossing. In this paper, we present a measure-

ment of the momentum deposited far from the jets in $\bar{p}p$ interactions at $\sqrt{s} = 1800$ and $\sqrt{s} = 630$ GeV and compare our measurement with the momentum observed in minimum bias events and with the predictions from two Monte Carlo models. The jet samples used in this analysis are the same as for the inclusive jet cross section measurements at the two center-of-mass energies. The study of *interjet* soft gluon radiation is also of special interest in QCD as its emission originates from the flow of color between jets. The analysis of such observables may lead to a better understanding of color neutralization [11,12].

The study reported in this paper is complementary to our previous analysis [13], which examined the evolution of event structure in low to moderate E_T events in $\bar{p}p$ interactions at $\sqrt{s} = 1800$ GeV by studying charged particle jets from 0.5 GeV/c to 50 GeV/c. The previous study found that the momentum transverse to the leading jet rises rapidly in the 0.5–5.0 GeV/c range and is almost constant when the leading charged particle jet has transverse momentum greater than about 10 GeV/c.

To study the underlying momentum in jet events, we define two cones with radius $R = \sqrt{(\Delta\eta)^2 + (\Delta\phi)^2} = 0.7$ centered at $\eta = \eta^{(1)}$, and $\phi = \phi^{(1)} \pm 90^0$ where $(\eta^{(1)}, \phi^{(1)})$ is the centroid of the highest energy jet in the event as shown in Fig. 1. The sum of the transverse momenta of all tracks in the two cones is labeled $P_T^{90,\min}$ and $P_T^{90,\max}$, where $P_T^{90,\max}$ is higher of the two values. By definition,

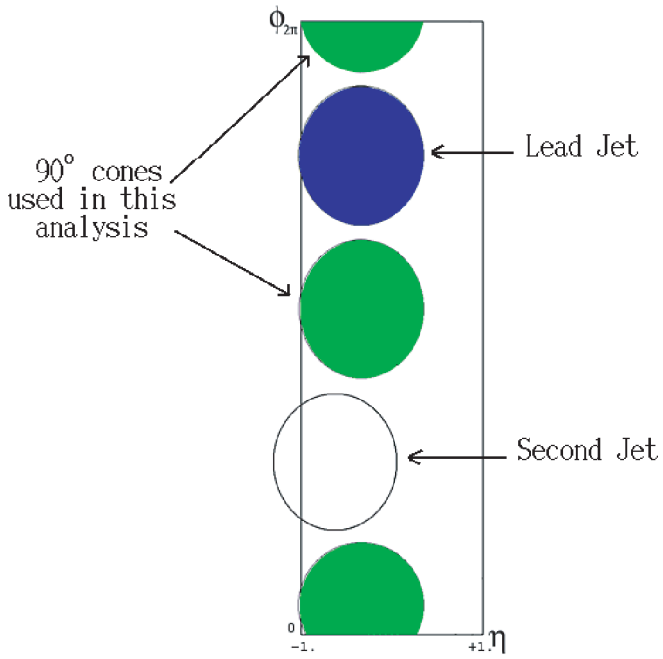

FIG. 1 (color online). An example of a 2-jet event in the detector region under study. The cones used for the determination of the underlying event contribution are at $\eta = \eta^{(1)}$ and $\phi = \phi^{(1)} \pm 90°$ where $(\eta^{(1)}, \phi^{(1)})$ is the centroid of the highest E_T jet in the event.

$P_T^{90,\max}$ should contain a larger contribution from initial and final state radiation than $P_T^{90,\min}$. In the approximation of a negligible four parton final state component, $P_T^{90,\min}$ is a measure of the underlying momentum in the jet event. In minimum bias data, we perform a similar analysis but with the cone centroid selected randomly in the central rapidity region, $|\eta| < 0.5$. We also use a second procedure, the *Swiss cheese* method, in which the transverse momenta of all the tracks except those in the two or three highest energy jets are summed and compared with Monte Carlo generator predictions and minimum bias data. A study of this type was first suggested in Ref. [14].

The data were collected using the CDF detector [15] with the Fermilab Tevatron Collider at $\sqrt{s} = 1800$ GeV (1994–1995) and $\sqrt{s} = 630$ GeV (1995). The CDF detector is a multipurpose detector consisting of a tracking system in a solenoidal magnetic field, calorimeters, muon chambers and two arrays of scintillator counters (BBC) located at ± 5.8 m from the nominal interaction point along the beam direction, covering the $3.2 \leq |\eta| \leq 5.9$ region. Minimum bias events were triggered by a coincidence of hits in these counters. The BBC cross section is 51.15 ± 1.60 mb compared to a total inelastic cross section for $\bar{p}p$ interactions of 60.33 ± 1.40 mb at $\sqrt{s} = 1800$ GeV [16]. The jet data were collected using four triggers requiring a cluster of energy in the calorimeter with $E_T \geq 20$, 50, 70 and 100 GeV at $\sqrt{s} = 1800$ GeV. These data samples, and the jet clustering and energy corrections have been described in detail in [1]. The data at $\sqrt{s} = 630$ GeV employed two triggers requiring a cluster with $E_T \geq 5$ and 15 GeV, respectively. The jet energies were corrected for any energy loss in the detector. At both energies we use only those events in which the centroid of the highest energy jet is within the central rapidity region, $|\eta| < 0.5$.

The tracking system consists of a silicon vertex detector (SVX′), a vertex tracking chamber (VTX), and a central tracking chamber (CTC) [17]. The vertex reconstruction is performed using information from the VTX and the CTC. In this analysis, the jet events were required to have one and only one primary vertex of high quality (corresponding to a high track multiplicity). For inclusive jet analyses in general, there is no restriction on the number of vertices as long as there is at least one high quality vertex. The one vertex requirement in this analysis is implemented in order to restrict the events to those in which only one interaction occurred during that beam crossing. For minimum bias data, the requirement is changed to one vertex of medium quality (corresponding to a lower minimum track multiplicity, but one resulting from beam-beam rather than beam-gas interactions).

Track reconstruction takes place primarily using hit information from the CTC. In order to ensure a high quality for the reconstructed tracks, each track is required to have at least four hits in each of the five axial super-

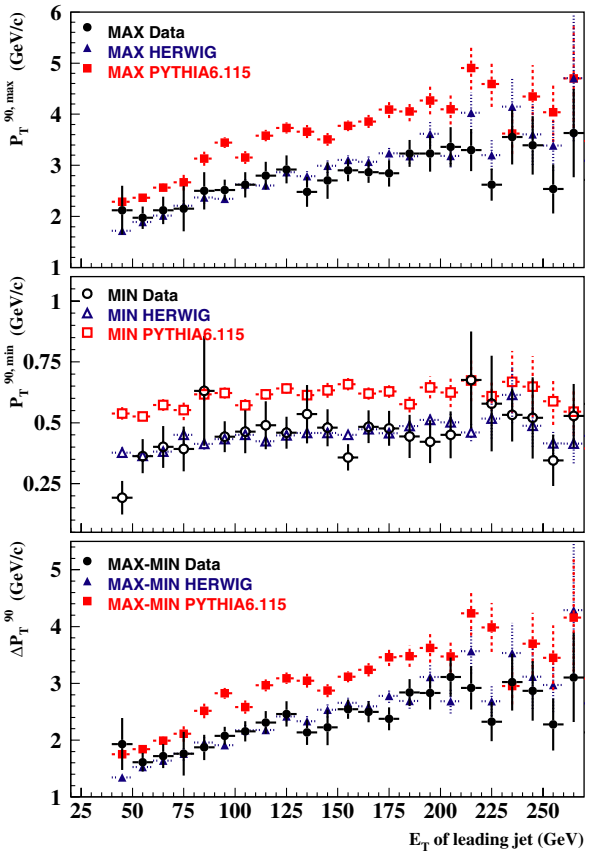

FIG. 2 (color online). $P_T^{90,\mathrm{max}}$, $P_T^{90,\mathrm{min}}$ and their difference ΔP_T^{90} as a function of the E_T of the highest energy jet at $\sqrt{s} = 1800$ GeV. The default parameters for PYTHIA (version 6.115) and HERWIG (version 5.6) have been used.

layers and hits in at least one stereo superlayer. The momentum resolution in the rapidity region $|\eta| \leq 1$ is better than $\delta P_T/P_T^2 \leq 0.002\ (\mathrm{GeV/c})^{-1}$. We require the tracks to have $P_T \geq 0.4$ GeV/c and to be within 5 cm in the longitudinal and 0.5 cm in the transverse direction of the $\bar{p}p$ vertex. The uncertainty on the quantities measured in this analysis is evaluated by loosening these cuts to 10 cm and 5 cm, respectively. The charged track reconstruction efficiency is uniform in rapidity for $|\eta| \leq 1$ and is on average $\sim 92 \pm 3\%$ [18]. The efficiency drops to 80% at low P_T (0.4–0.5 GeV/c) and to 60% in the region $1.0 \leq |\eta| \leq 1.2$. We correct the data for the inefficiency in both regions. The main systematic uncertainty in our analysis arises from the track selection criteria and from the track reconstruction efficiency. The data were compared to Monte Carlo generator predictions from the programs HERWIG (version 5.6) [19] and PYTHIA (version 6.115) [20]. At $\sqrt{s} = 1800$ GeV, four samples of jet events were generated with HERWIG and PYTHIA, with a minimum transverse momentum for the hard scattering of 20, 40, 60 and 80 GeV, for the four samples. The leading jet in the generated distributions was required to have a transverse energy of 40, 75, 100 and 130 GeV, respectively. The output from both Monte Carlo programs consists of the 4-vectors of the final state hadrons. For comparison to the Monte Carlo generator predictions, the data were corrected for the track reconstruction efficiency.

In Fig. 2, a comparison of the $P_T^{90,\mathrm{max/min}}$ distributions between data and Monte Carlo is shown. $P_T^{90,\mathrm{max}}$ increases as the leading jet E_T increases, both in the data and in the Monte Carlo generator predictions. The $P_T^{90,\mathrm{min}}$ distributions are almost independent of $E_T^{(1)}$ indicating that any contribution from higher order radiation, at least in this $\eta - \phi$ region, is small. Both the Monte Carlo generator predictions and the data show a similar behavior. The average values of $P_T^{90,\mathrm{max}}$ and $P_T^{90,\mathrm{min}}$ are given in Table I for different intervals of $E_T^{(1)}$, for the data and for the two Monte Carlo generators. Good agreement is observed with HERWIG, while PYTHIA lies above the data. The parameters of the underlying event model in PYTHIA can be adjusted more easily than those in HERWIG. We

TABLE I. Average P_T inside the max and min cone at $\eta = \eta^{(1)}$ and $\phi = \phi^{(1)} \pm 90°$ for $\sqrt{s} = 1800$ GeV data. In data, the first errors shown are statistical and the second are systematic.

$E_T^{(1)}$ (GeV)	DATA	HERWIG 5.6	PYTHIA 6.115 (default)	PYTHIA 6.115 (tuned)
		$P_T^{90,\mathrm{max}}$ (GeV/c)		
40–80	$2.04 \pm 0.09 \pm 0.21$	1.92 ± 0.04	2.43 ± 0.04	2.19 ± 0.04
80–120	$2.64 \pm 0.09 \pm 0.19$	2.49 ± 0.05	3.39 ± 0.06	2.96 ± 0.06
120–160	$2.89 \pm 0.09 \pm 0.22$	2.95 ± 0.05	3.69 ± 0.06	3.56 ± 0.06
160–200	$3.27 \pm 0.10 \pm 0.22$	3.21 ± 0.07	4.02 ± 0.09	3.93 ± 0.09
200–270	$3.64 \pm 0.21 \pm 0.24$	3.59 ± 0.16	4.35 ± 0.17	4.24 ± 0.19
		$P_T^{90,\mathrm{min}}$ (GeV/c)		
40–80	$0.37 \pm 0.03 \pm 0.06$	0.38 ± 0.01	0.54 ± 0.01	0.38 ± 0.01
80–120	$0.47 \pm 0.02 \pm 0.07$	0.43 ± 0.01	0.61 ± 0.01	0.44 ± 0.01
120–160	$0.42 \pm 0.02 \pm 0.06$	0.45 ± 0.01	0.64 ± 0.01	0.48 ± 0.01
160–200	$0.46 \pm 0.02 \pm 0.06$	0.48 ± 0.01	0.62 ± 0.02	0.53 ± 0.02
200–-270	$0.53 \pm 0.05 \pm 0.07$	0.50 ± 0.02	0.63 ± 0.03	0.53 ± 0.04

TABLE II. The Monte Carlo generators default and tuned parameters. MSTP(82) defines the structure of the multiple parton interactions; PARP(82) is the regularization scale of the transverse momentum spectrum for multiple interactions (with MSTP(82) ≥ 2); PARP(85) and PARP(86) are the probability that the multiple interaction produces two gluons with color connections to the nearest neighbors (or as a closed gluon loop) [20].

	PYTHIA			HERWIG
	default 6.115 1800 and 630 GeV	tuned 6.115 1800 GeV	tuned 6.115 630 GeV	default 5.6 1800 and 630 GeV
Parton distribution function	MRSG	CTEQ4L	CTEQ4L	CTEQ3L
MSTP(82)	1	3	3	···
PARP(82)	···	2.0 GeV/c	1.4 GeV/c	···
PARP(85)	0.33	1	1	···
PARP(86)	0.66	1	1	···

have attempted to reach a better agreement with the predictions from PYTHIA by using a more modern parton distribution function (CTEQ4L [21] instead of MRSG [22]), using the option of varying impact parameters with a matter distribution inside the hadron described by a simple Gaussian (MSTP(82) = 3), and by decreasing the regularization scale of the transverse momentum spectrum for multiple interactions (P_{T0}) to 2.0 GeV/c from the default value of 2.3 GeV/c. (Such a decrease causes the double-parton scattering component of the underlying event to be less hard, leading to a better agreement with the data.) Table II summarizes the Monte Carlo generators default and tuned parameters. The behavior of PYTHIA with the adjusted parameters can be observed in Fig. 3 and in the last column in Table I. The tuning leads to a better agreement with the data in the low $E_T^{(1)}$ region but leaves PYTHIA still somewhat larger in the high $E_T^{(1)}$ region.

In Fig. 4, the total charged track momentum in the two cones (min+ max) is shown for five different bins of $E_T^{(1)}$. The effects due to large angle (away from any jet) soft gluon emission are expected to be appreciable when the

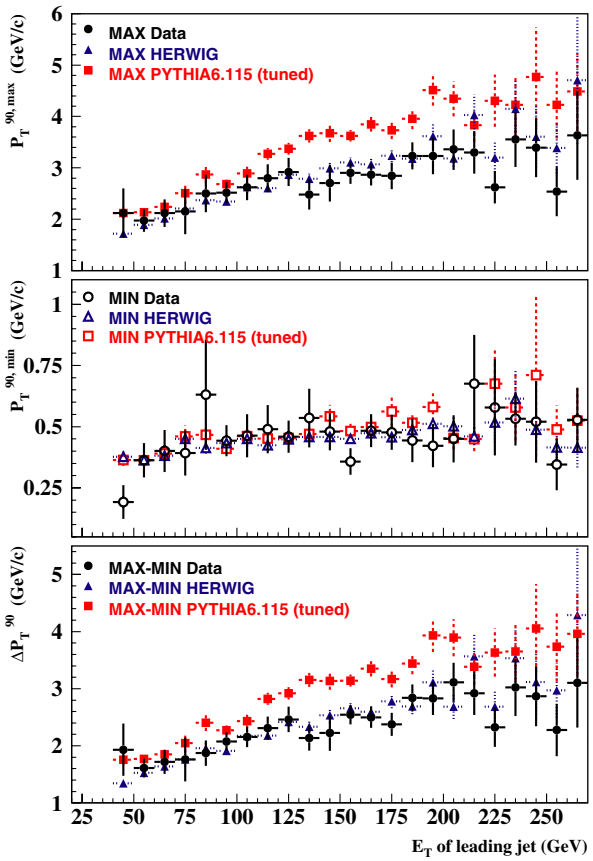

FIG. 3 (color online). $P_T^{90,\max}$, $P_T^{90,\min}$ and their difference ΔP_T^{90} as a function of the E_T of the highest energy jet at $\sqrt{s} =$ 1800 GeV. PYTHIA (version 6.115) has been tuned to reproduce the data. The default parameters for HERWIG (version 5.6) have been used.

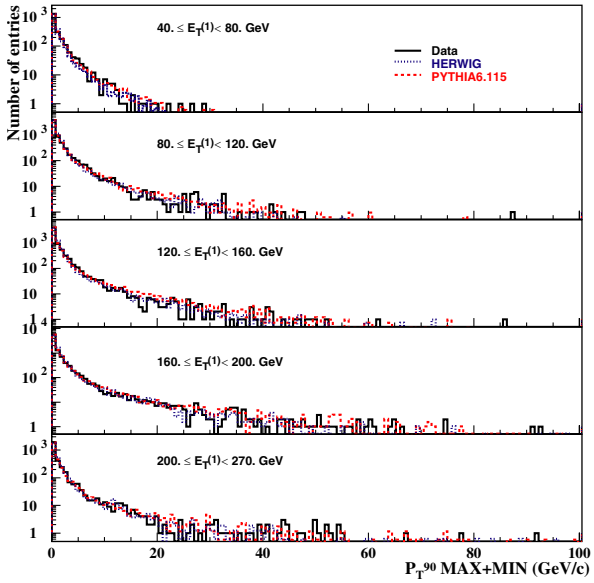

FIG. 4 (color online). The distributions for the total p_T in the sum of the max and min cones is plotted for five different bins of the E_T of the highest energy jet. Data, HERWIG (version 5.6) and PYTHIA (version 6.115) distributions are shown at $\sqrt{s} = 1800$ GeV.

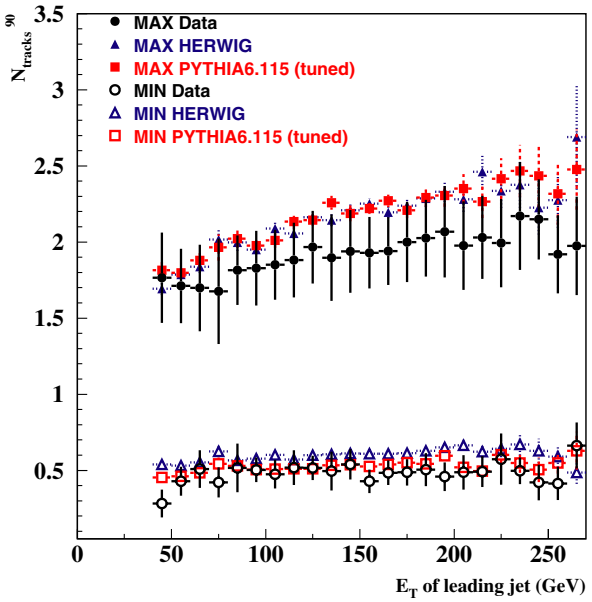

FIG. 5 (color online). Number of tracks in the max and min cone as a function of the E_T of the leading jet. Data, HERWIG (version 5.6) and PYTHIA (version 6.115) distributions are plotted at $\sqrt{s} = 1800$ GeV.

transverse momentum in the min+max cones ($p_T^{\max} + p_T^{\min}$) is larger than a few GeV and when the ratio of the lead jet transverse momentum to the transverse momentum in the cones is large. Such emissions are included in an approximate way in existing parton shower Monte Carlo generators and a detailed comparison may lead to improvements in their treatment [23]. Qualitatively, HERWIG and PYTHIA agree with the data, although the PYTHIA prediction tends to be slightly higher than the data for larger values of transverse momentum in the two cones [24].

The average number of tracks found inside the two cones is shown in Fig. 5, plotted as a function of $E_T^{(1)}$. A slightly higher track multiplicity is observed in both of the simulations compared to the data.

TABLE III. Mean $P_T^{MB,\text{cone}}$ and the mean number of tracks in a random cone of radius 0.7 in $\sqrt{s} = 1800$ GeV minimum bias data. Only systematic errors are shown. Statistical errors are less than 0.5%.

		$P_T^{MB,cone}$ (GeV/c)	Track Multiplicity
DATA	all vertices	0.36 ± 0.04	0.45 ± 0.06
	high quality vertex	0.57 ± 0.06	0.69 ± 0.09
HERWIG		0.31	0.44
PYTHIA (tuned)		0.35	0.44

In Table III, the mean values of the total track P_T and the mean number of tracks inside a cone randomly placed in the region $|\eta| \leq 0.5$ are shown for all minimum bias events and for those with a high quality vertex only. For the entire sample, the mean transverse momentum ($P_T^{MB,\text{cone}}$) in the cone is about 0.36 ± 0.04 GeV/c, while restricting the sample to events having a high quality vertex, the transverse momentum increases to 0.57 ± 0.06 GeV/c. The average for the $P_T^{90,\min}$ cone over the measured $E_T^{(1)}$ range is approximately 0.45 GeV/c, or midway between the above values.

The total event track multiplicity and track momentum distributions in minimum bias data in the region $|\eta| < 0.7$ are shown in Fig. 6, with the number of entries in the simulation normalized to the number in the data. The transverse momentum distribution at high P_T is not well-reproduced by HERWIG, which has virtually no tracks with $P_T \geq 4$ GeV/c. The absence of high P_T tracks indicates the lack of a semihard processes in the HERWIG model of minimum bias events. In contrast, PYTHIA reproduces the transverse momentum distribution considerably better. The model of multiple parton interactions incorporated in the PYTHIA description of minimum bias events [25] allows for the possibility of

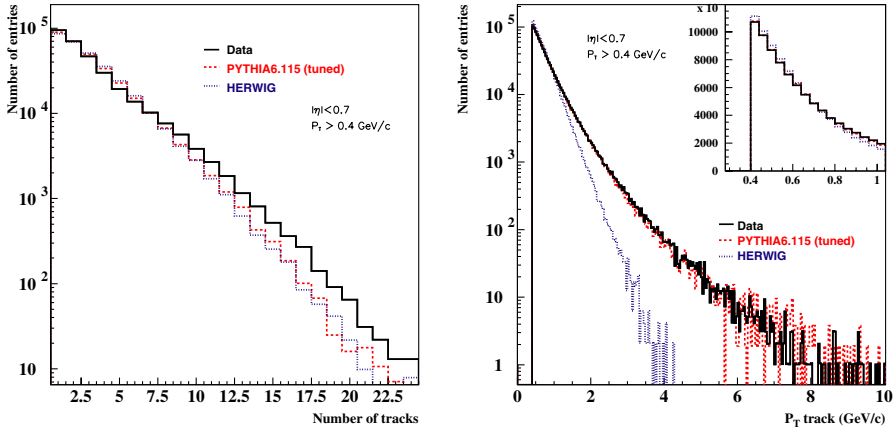

FIG. 6 (color online). Distribution of track multiplicity (left) and transverse momentum (right) in the $\sqrt{s} = 1800$ GeV minimum bias sample. The inset in the right plot shows the low P_T portion of the spectrum on a linear scale.

high transverse momentum tracks. Neither HERWIG nor PYTHIA appears to correctly describe the high multiplicity end of the track multiplicity distribution.

As previously described, the *Swiss cheese* distribution is formed by summing the transverse momentum of the tracks in the central region ($|\eta| \leq 1$), excluding the transverse momentum of the tracks in a radius 0.7 from the center of the two (or three) most energetic jets in the event (where an E_T requirement of 5 GeV has been placed on each jet).

The sum of the track transverse momentum in the central region for the 2-jet subtracted and 3-jet subtracted distributions is shown in Fig. 7 for the data, HERWIG and the version of PYTHIA tuned for best agreement with the max/min cone data. In the simple picture presented earlier, the difference between the *Swiss cheese* level with the two highest E_T jets subtracted and the corresponding minimum bias level should be proportional to the NLO (third parton) and higher order contributions. The *Swiss cheese* level with the three highest E_T jets subtracted should have little or no NLO contribution. Both the 2-jet subtracted and 3-jet subtracted distributions increase as the lead jet E_T increases, with the slope being less for the 3-jet subtracted case. The 3-jet subtracted *Swiss cheese* average P_T/(unit $\eta - \phi$) is 0.92 ± 0.09 GeV/c compared to 0.37 ± 0.04 GeV/c observed in minimum bias data with high quality vertices and 0.23 ± 0.04 GeV/c in all minimum bias events. The larger momentum observed in the 3-jet subtracted *Swiss cheese* distribution indicates additional contributions than just those from the soft underlying event. These contributions include hadronization from the jets (*splashout*), double-parton scattering, higher order radiation effects [26], as well as contributions from third jets that fail the E_T threshold cut of 5 GeV. For comparison, the average momentum/(unit $\eta - \phi$) in the min(max) cone is 0.29 ± 0.04 (1.91 ± 0.14) GeV/c.

To study the energy dependence, we have analyzed jet and minimum bias data at $\sqrt{s} = 630$ GeV. In Fig. 8, $P_T^{90,\mathrm{max}}$ and $P_T^{90,\mathrm{min}}$ (and their difference) are plotted as a function of $E_T^{(1)}$. The $\sqrt{s} = 630$ GeV data shows a similar behavior as was observed at $\sqrt{s} = 1800$ GeV but the overall magnitudes are lower. The average $P_T^{90,\mathrm{min}}$ ($P_T^{90,\mathrm{max}}$) at $\sqrt{s} = 630$ GeV is $0.25 \pm 0.04 (1.43 \pm 0.12)$ GeV/c, $\sim 0.2 (\sim 1.5)$ GeV/c lower than what is observed at $\sqrt{s} = 1800$ GeV. Both HERWIG and the tuned PYTHIA reproduce the data at 630 GeV well. PYTHIA has been tuned as for the analysis at 1800 GeV, but with the regularization scale, P_{T0}, set to 1.4 GeV/c. A dependence of P_{T0} on the center of mass energy has been implemented in versions of PYTHIA after 6.12 according to the model described in [27]. This model, however, predicts a value for P_{T0} of 1.9 GeV/c for the 630 GeV data while in the 1800 GeV

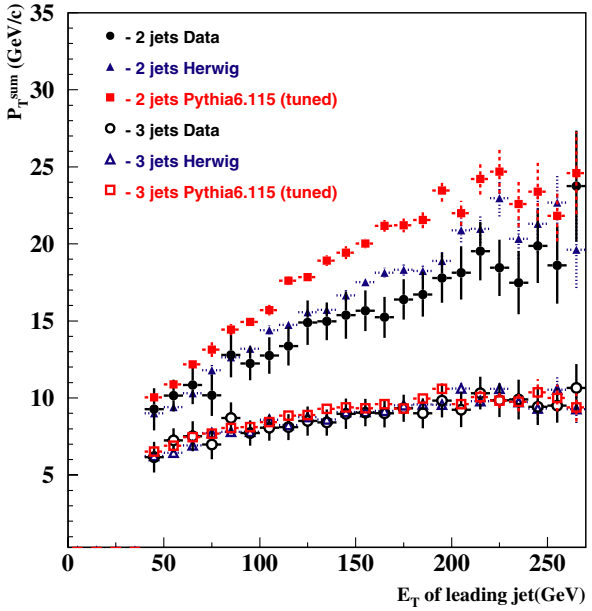

FIG. 7 (color online). P_T^{sum} (*Swiss cheese*). The two and three most energetic jets in each event are subtracted from the total transverse momentum in the central detector region. Data, HERWIG (version 5.6) and PYTHIA (version 6.115) results are shown at $\sqrt{s} = 1800$ GeV.

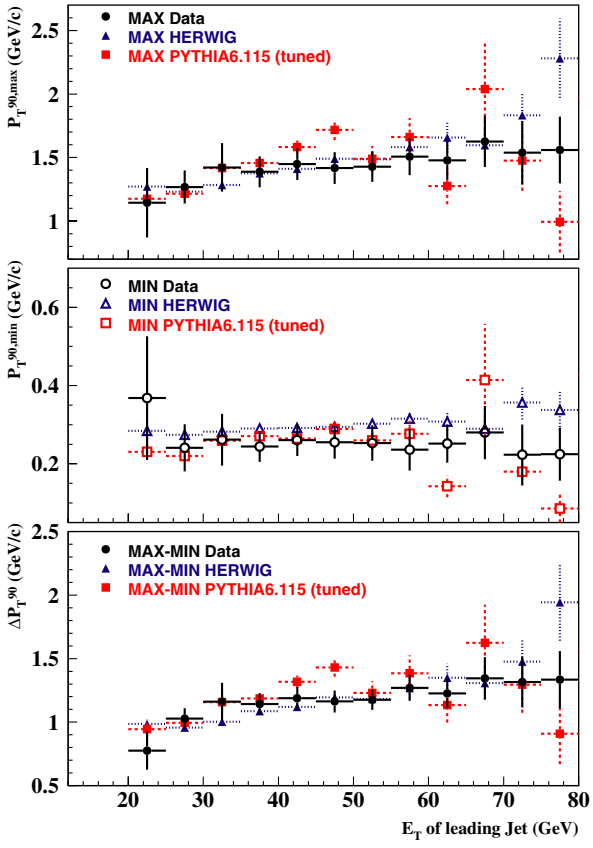

FIG. 8 (color online). $P_T^{90,\mathrm{min}}$, $P_T^{90,\mathrm{max}}$ and their difference ΔP_T^{90} at $\sqrt{s} = 630$ GeV as a function of the E_T of the leading jet.

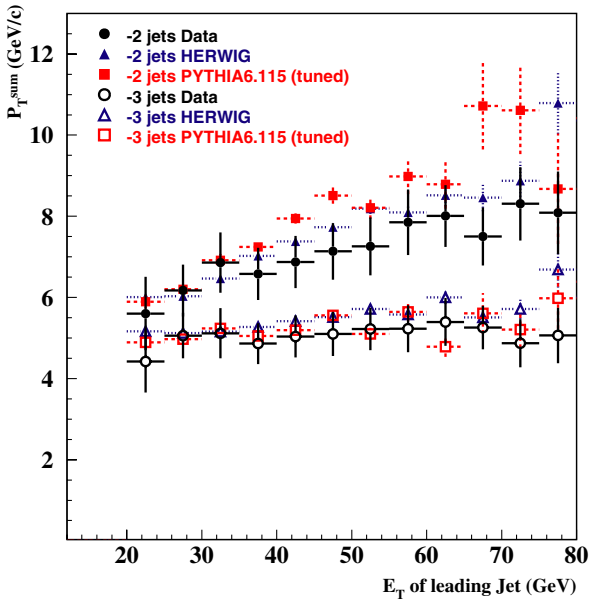

FIG. 9 (color online). P_t^{sum} (*Swiss cheese*). The two and three most energetic jets in the events are subtracted from the total transverse momentum in the central detector region. Data, HERWIG (version 5.6) and PYTHIA (version 6.115) results are shown at $\sqrt{s} = 630$ GeV.

data the prediction is 2.3 GeV/c, showing a smaller dependence on the center-of-mass energy than that observed in our data. Using the default values the PYTHIA predictions underestimates the number of charged particles at $\sqrt{s} = 630$ GeV.

The *Swiss cheese* distributions at 630 GeV are shown in Fig. 9. A very good agreement between data and both Monte Carlo generators is observed if the three most energetic jets are subtracted. In the case where the two most energetic jets are subtracted, both Monte Carlo generators lie above the data, as was also observed at

TABLE IV. Data and simulation comparisons for minimum bias events at $\sqrt{s} = 630$ GeV. Average $P_T^{MB,cone}$ and the average number of tracks in a random cone of radius 0.7 are shown. Only systematic errors are shown. Statistical errors are less than 0.2%.

		$P_T^{MB,cone}$ (GeV/c)	Track Multiplicity
DATA	all vertices	0.29 ± 0.03	0.37 ± 0.05
	high quality vertex	0.52 ± 0.05	0.65 ± 0.08
HERWIG		0.26	0.36
PYTHIA		0.28	0.38

1800 GeV. Again, the momentum is larger when 3-jets are subtracted (P_T/(unit $\eta - \phi$) is 0.52 ± 0.05 GeV/c) than in minimum bias events with a high quality vertex(P_T/(unit $\eta - \phi$) is 0.34 ± 0.03 MeV/c).

In Table IV are shown the average value of the total track P_T and the mean number of tracks inside a cone in the central rapidity region in minimum bias data at $\sqrt{s} = 630$ GeV. The sum of the track transverse momenta is 20% (10%) lower with respect to the 1800 GeV data for the sample with all vertices (high quality vertex only). Figure 10 shows the track multiplicity and momentum distributions for minimum bias events. Again, the number of entries in the simulation is normalized to the number of entries in the data. The track multiplicity distribution and the mean $P_T^{MB,\text{cone}}$, dominated by the low edge of the steeply falling spectrum, is well-reproduced by both Monte Carlo generators. Unlike the situation at 1800 GeV, PYTHIA fails to produce enough high P_T tracks, although it still produces considerably more than HERWIG.

In summary we have studied the momentum deposited in two cones at $\pm 90°$ to the highest E_T jet in hard interaction events at $\sqrt{s} = 1800$ and 630 GeV. The maximum of the two cone energies increases with highest E_T

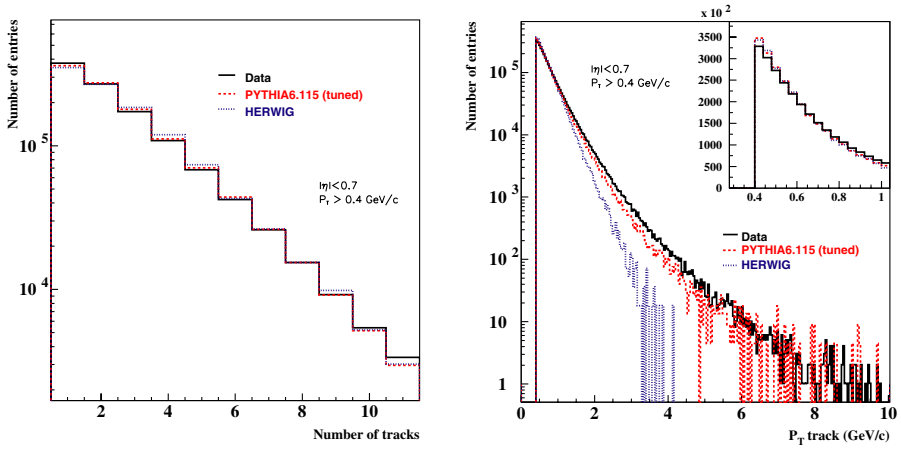

FIG. 10 (color online). Distribution of track multiplicity (left) and transverse momentum (right) in the $\sqrt{s} = 630$ GeV minimum bias sample. The inset in the right plot shows the low P_T portion of the spectrum on a linear scale.

jet in the event whereas the minimum is flat. Both HERWIG and PYTHIA exhibit the same behavior but HERWIG provides a better description of the CDF data. The momentum in the min cone is midway between the levels observed in generic minimum bias events and minimum bias events selected by high track multiplicity. In the HERWIG minimum bias model, the generated tracks are too soft, and semihard or hard interactions should be added to the minimum bias events in order to better reproduce the data. PYTHIA, however, with an adequate tuning of its parameters, reproduces the charged particle distribution better than HERWIG for the 1800 GeV minimum bias data, but is less successful at 630 GeV. We have measured the $\sqrt{s}$ dependence of the underlying event momentum in jet events and ambient energy in minimum bias events. The underlying momentum at $\sqrt{s} = 630$ GeV is 45% lower than what is observed in 1800 GeV data. These measurements will allow for more precise tunings of both the underlying event in Monte Carlo programs and the mechanisms for gluon radiation, help to reduce the uncertainties in future jet studies at the Tevatron and will lead to a better prediction of physics signals and backgrounds at the Large Hadron Collider.

We thank the Fermilab staff and the technical staffs of the participating institutions for their vital contributions. This work was supported by the U.S. Department of Energy and National Science Foundation; the Italian Istituto Nazionale di Fisica Nucleare; the Ministry of Education, Culture, Sports, Science and Technology of Japan; the Natural Sciences and Engineering Research Council of Canada; the National Science Council of the Republic of China; the Swiss National Science Foundation; the A. P. Sloan Foundation; the Bundesministerium fuer Bildung und Forschung, Germany; the Korean Science and Engineering Foundation and the Korean Research Foundation; the Particle Physics and Astronomy Research Council and the Royal Society, UK; the Russian Foundation for Basic Research; the Comision Interministerial de Ciencia y Tecnologia, Spain; in part by the European Community's Human Potential Programme under Contract No. HPRN-CT-20002, Probe for New Physics; and by the Research Fund of Istanbul University Project No. 1755/21122001.

[1] CDF Collaboration, Phys. Rev. D **64**, 032001 (2001).
[2] CDF Collaboration, Phys. Rev. Lett. **77**, 438 (1996).
[3] CDF Collaboration, Phys. Rev. Lett. **68**, 1104 (1992).
[4] D0 Collaboration, Phys. Rev. Lett. **82**, 2451 (1999).
[5] D0 Collaboration, Phys. Rev. Lett. **86**, 1955 (2001).
[6] D0 Collaboration, Phys. Rev. Lett. **86**, 1707 (2001).
[7] D0 Collaboration, Phys. Rev. D **64**, 032003 (2001).
[8] D0 Collaboration, Phys. Rev. D **67**, 052001 (2003).
[9] CDF Collaboration, A. Bhatti, in*Proceedings of the 9th Meeting of the Division of Particles and Fields of the American Physical Society, Minneapolis, 1996*, edited by K. Heller, J. K. Nelson, and D. Reeder (World Scientific, Singapore, 1998), p. 483.
[10] D0 Collaboration, Phys. Rev. Lett. **86**, 2523 (2001).
[11] A. Banfi, G. Marchesini, G. Smye, J. High Energy Phys. 0208 (2202) 006.
[12] M. Dasgupta and G. P. Salam, J. High Energy Phys. 0203 (2002) 017.
[13] CDF Collaboration, Phys. Rev. D **65**, 092002 (2002).
[14] G. Marchesini and B. R. Webber, Phys. Rev. D **38**, 3419 (1988).
[15] CDF Collaboration, Nucl. Instrum. Methods Phys. Res., Sect. A **271**, 387 (1998).
[16] CDF Collaboration, Phys. Rev. Lett. **76**, 3070 (1996).
[17] CDF Collaboration, Nucl. Instrum. Methods Phys. Res., Sect. A **265**, 1 (1988).
[18] CDF Collaboration, Phys. Rev. D **58**, 072001 (1998).
[19] HERWIG, G. Marchesini, B. R. Webber, G. Abbiendi, I. G. Knowles, M. H. Seymour, L.Stanco, Comput. Phys. Commun. **67**, 465 (1992).
[20] T. Sjöstrand, Comput. Phys. Commun. **82**, 74 (1994).
[21] CTEQ Collaboration, Phys. Rev. D **55**, 1280 (1997).
[22] A. D. Martin, W. J. Stirling, and R. G. Roberts in *Parton Distribution Functions*, MRS Symposia Proceedings No. 021 (Materials Research Society, Pittsburgh, 1995).
[23] G. Marchesini (private communication).
[24] For many related observables, a better agreement of PYTHIA predictions with CDF data has subsequently been obtained using a specific variation of the PYTHIA parameters known as Tune A; see www.phys.ufl.edu/rfield/cdf/tunes/rdf_tunes.html.
[25] T. Sjöstrand and M. van Zijl, Phys. Rev. D **36**, 2019 (1987).
[26] J. Pumplin, Phys. Rev. D **57**, 5787 (1998).
[27] T. Sjöstrand, L. Lönnblad, S. Mrenna, hep-ph/0108264.